



Influence of the thickness of a nonmagnetic layer on the coupled dynamics of magnetic vortices in a spin-transfer nanooscillator

V. V. Mukhamadeeva^{†,1}, S. V. Stepanov¹, K. A. Zvezdin^{2,3}, E. G. Ekomasov¹

[†]mukhamadeeva.vika@mail.ru

¹Bashkir State University, Ufa, 450076, Russia

²Prokhorov General Physics Institute of the RAS, Moscow, 119991, Russia

³New Spintronic Technologies, Russian Quantum Center, Moscow, 143026, Russia

A spin torque nano-oscillator in the form of a three-layer magnetic tunneling junction of small diameter (120 nm), where the magnetizations in both magnetic layers are in vortex state, is considered. The effect of the thickness of a nonmagnetic layer on the coupled dynamics of two magnetic vortices in a spin torque nano-oscillator has been studied. The thick permalloy magnetic layer has a thickness of 15 nm, the middle non-magnetic layer has a thickness in the first case of 12.5 and in the second 15 nm, and the thin permalloy magnetic layer has a thickness of 4 nm. Numerical calculation of the dynamics of magnetostatically coupled vortices was carried out using the software package SpinPM for micromagnetic modeling. The features of the vortex motion dynamic are studied for different thicknesses of the nonmagnetic interlayer. It is shown that in all cases of thickness of the nonmagnetic interlayer, three regimes of vortex dynamics are observed: the oscillations of magnetic vortices damped over time, the mode of stationary coupled oscillations of magnetic vortices, and regime, when vortices “leave” the edge of the disk. It is found that increasing in the thickness of the nonmagnetic layer leads to decreasing in the values of the first, second, and third critical currents.

Keywords: magnetic vortices, nonlinear dynamics, magnetic nanodiscs, spintronics.

1. Introduction

Vortex spin torque nano-oscillators (STNOs) are three-layer nanodisks in which the magnetic layers (one or both) contain a magnetic vortex [1]. Interest in the study of vortex STNOs is associated with great prospects for their practical applications and some advantages over conventional STNOs [1, 2–5]. In vortex STNOs, a high microwave signal power and a relatively narrow line width were achieved [1]. There are different types of magnetic vortices. In addition to the usual circular vortex and anti-vortex, there is also known a radial vortex and a curled vortex [1, 6]. The magnetic structure of the circular vortex located in the center of the disk under equilibrium conditions looks qualitatively as follows: the magnetization field lies in a plane and twists around the center of the vortex. In a small surrounding of the disk center, the magnetization leaves the plane and is oriented perpendicular to it. This central part is called the core of the vortex and has a diameter of about 10 nm. It is known that in permalloy nanodisks a magnetic circular vortex can be realized as the ground state [1, 2]. A special C-state when vortex is partially “squeezed” out of the disk has been demonstrated [5]. These micromagnetic structures attract significant interest of researchers, as they can be much smaller than ordinary vortex ones and demonstrate interesting dynamic properties [5, 7]. There are many experimental and theoretical papers devoted to the study of the magnetostatically bounded magnetic vortices dynamics [8–17]. It turned out that for a system where both magnetic

layers are in a vortex state and each of them act as a polarizer and as a free layer at the same time, the spectrum line width decreases dramatically [15, 16] in comparison to the single vortex spin-torque nanooscillators [1, 16]. The properties of such system largely depend on the mutual orientation of the vortex cores [11, 16, 17]. Using a spin-polarized current and an external magnetic field, the coupled dynamics and structure of vortices can be controlled [1, 12, 17–21]. Promising in the context of practical applications is the use of a stationary moving vortex and switching its polarity and/or chirality [1].

Previously, we considered the influence of the STNO diameter on the coupled dynamics of vortices under the action of a spin-polarized current [1, 12, 17, 21]. The existence of several critical values of currents separating different modes of vortex dynamics was found. However, the influence of the thickness of the nonmagnetic layer on the dynamics of coupled vortices has not yet been studied in detail. For example, in [10], its effect on the frequency of coupled vortex dynamics was theoretically studied only for the stationary regime of oscillations. For coupled vortices, it is of practical interest to study the dependence of the diameter of the STNO nonmagnetic layer on the spatiotemporal change in their position and structure, the trajectory of motion, and the time it takes for the system to enter different dynamic modes. In this work, the influence of the thickness of the nonmagnetic interlayer and the magnitude of the spin-polarized current on the features of the coupled dynamics of magnetic vortices in nanodisks with a small diameter of 120 nm have been theoretically studied.

2. Model and computational procedure

To describe the nonlinear dynamics of the magnetization vector \mathbf{M} in each of the STNO magnetic layers the generalized Landau-Lifshitz equation (LLE) is used [1]:

$$\dot{\mathbf{M}} = -[\mathbf{M} \times \mathbf{H}_{\text{eff}}] + \frac{\alpha}{M_s} [\mathbf{M} \times \dot{\mathbf{M}}] + \mathbf{T}_{\text{s.t.}}, \quad (1)$$

where M_s is the saturation magnetization, and α is the Hilbert damping parameter. The effective field \mathbf{H}_{eff} is the sum of the external magnetic field \mathbf{H}_{ext} , Oersted magnetic field \mathbf{H}_{Oe} , the fields of magnetostatic, anisotropic and exchange interactions (see Eq. (2)). $\mathbf{T}_{\text{s.t.}}$ is the additional torque [1] responsible for the interaction of the spin-polarized current with the magnetization (see Eq. (3), (4)).

$$\mathbf{H}_{\text{eff}} = \frac{2A}{M_s^2} \Delta \mathbf{M} + \frac{2K}{M_s^2} (\mathbf{M}, \mathbf{n}) \mathbf{n} + \int_V \text{div} \mathbf{M}(\mathbf{r}_1) \frac{r - r_1}{|r - r_1|^3} d\mathbf{r}_1 + \mathbf{H}_{\text{ext}} + \mathbf{H}_{\text{Oe}}, \quad (2)$$

$$\mathbf{T}_{\text{s.t.}} = \frac{\gamma a_j}{M_s} \mathbf{M} \times [\mathbf{M} \times \mathbf{m}_{\text{ref}}] + \gamma \mathbf{b}_j \mathbf{M} \times \mathbf{m}_{\text{ref}}, \quad (3)$$

$$a_j = \frac{\hbar}{2|e|d} P \frac{1}{M_s} J_e, \quad b_j = \beta a_j, \quad \beta \approx 0.05 - 0.2, \quad (4)$$

here A is exchange interaction constant, K is anisotropy constant, \mathbf{n} is normal vector, \mathbf{r} is radius vector, \hbar is Planck's constant, e is the electron charge, d is the thickness of the magnetic layer, J_e is the current density, P is the current polarization, γ is the gyromagnetic ratio. It should be noted that in this work, the dynamics of the magnetization of both magnetic layers was modeled; therefore, \mathbf{m}_{ref} is inhomogeneous in space, and depends on time and is determined by numerically solving the LLG equation in the entire system. This simulation approach has already been used in our previous work [12,17,20,21]. LLE is a complex integro-differential equation and the number of analytical methods applications for its solution is very limited.

Many software packages have been developed for numerical calculations of magnetic structures, for example, OOMMF, mumax3, SPINPM [11,22,23]. To numerically calculate the structure and associated dynamics of magnetic vortices, micromagnetic modeling is going to be applied using the SpinPM package [11,12]. SpinPM micromagnetic code is based on the fourth-order Runge-Kutta method with adaptive time control for time integration and a grid size of $2 \times 2 \text{ nm}^2$. It allows you to study the remagnetization of a separate layer, to visualize the movements of the vortex, get the trajectories of its movements along the sample. This package is proved to be an effective tool to numerical investigation of bound vortices dynamics (see e.g. [12,17,20,21]).

Let us further take a look on the previously studied [11,12] three-layer nanodisks with a diameter of 120 nm. The thick magnetic layer made of permalloy ($\text{Ni}_{80}\text{Fe}_{20}$) has a thickness of 15 nm, thin — 4 nm. The magnetic parameters of the layers are taken the same as in the experimental work [11]:

$M_s = 700 \text{ Erg/Gs} \times \text{cm}^3$ for a “thick” and $M_s = 600 \text{ Erg/Gs} \times \text{cm}^3$ for a “thin” magnetic layer, exchange rigidity $A = 1.2 \cdot 10^{-6} \text{ Erg/cm}$ for “thick” and $A = 1.12 \cdot 10^{-6} \text{ Erg/cm}$ for “thin” layer, Hilbert's damping constant $\alpha = 0.01$, gyromagnetic ratio $\gamma = 2.0023 \cdot 10^7 \text{ rad/(T} \cdot \text{s)}$. The dynamics of the system strongly depends on the polarities of the vortices. For definiteness, it was assumed that the current polarization is $P = 0.1$, the current flows from bottom to top, from a thick layer to a thin one. At the initial moment of time, the vortex chirality in both magnetic layers is the same and corresponds to the direction of clockwise rotation. The direction of magnetization in the vortex cores is the same and is directed upwards.

The magnetization dynamics was modeled simultaneously in the whole nanopillar, in both magnetic layers. The thick layer was numerically splitted into three sub-layers in vertical direction, while the thin layer was simulated without splitting it into sublayers. We considered dynamics of two vortices on equal basis, which means that thin layer acts as a spin polarizer for the thick one and vice versa, both the vortex are moving, and the full-scale magnetostatic interaction between the layers is considered.

3. Results and discussion

Next, we investigated the dynamics and transformation of the structure of the initial vortices under the action of a spin polarized current. As shown earlier [12], there are three such critical current values for a layer thickness of 10 nm. The first of them limits the region of damped oscillations of magnetic vortices. The second of them limits the region of bound stationary oscillations of magnetic vortices. In this region, the oscillation frequency is practically independent of the current value, and the radii of the vortex orbits increase linearly with an increase in the current value. The third one restricts the area of “leaving” of the vortex from the thin magnetic layer. The thickness of the magnetic disc doesn't affect much the vortex structure, however the critical current at which the vortex polarity is switched depends on it strongly [22], thus a difference in thicknesses of magnetic layers in our case results in significant difference of the corresponding critical currents.

Let us examine nanopillars with a nonmagnetic interlayer 12.5 and 15 nm thick. For the trajectory of the vortex, we take the trajectory of the center of the vortex. The vortex center is the point at which the magnetization component perpendicular to the plane of the nanopillar has a maximum value. In the case when the current is less than the first critical value, when the current is turned on, both vortices move counter clockwise. The vortices move along a complex trajectory. The orbit broadens until it attains its maximum possible value. Then the motion is damped. The orbit radius of vortex motion in the thick layer is larger than in the thin layer and its maximum value is several nanometers. The time for which this regime lasts depends on the current strength. In our case, this time is about 5 – 20 nanoseconds.

At currents over the first critical value, both vortices move in the same direction with acceleration upon switching on the current and the orbits of their motion gradually increase. At the initial stage of motion, in the range from 0 to 5 ns, the motion is strongly nonstationary. Then the trajectory turns

to a helix. When the stationary motion regime is established, i.e., in about 20–60 ns from the beginning of motion, the polar angles of vortices moving in the thick and thin layers (these angles are determined by the straights passing through the core centers) are equal. The time for which the stationary regime is established depends on the current strength and in our case has a value of 70–80 ns.

Figures 1 and 2 show the dependences of the frequencies of the coupled oscillations of the vortices and the radius of their orbits on the magnitude of the current. It can be seen, as in the case of a non-magnetic interlayer of 10 nm, that there are critical values of the current that change the oscillation mode. The radius of the orbit of stationary motion of a vortex in a thick layer is also noticeably larger than in a thin one. The radius of the orbit of stationary motion in a thin magnetic layer for all cases first increases to a maximum value, then, when the second critical current is reached, it is zeroed due to the vortex core going beyond the edge of the STNO boundary. With an increase in the thickness of the non-magnetic layer,

the maximum radius of stationary motion of a vortex in a thin magnetic layer is almost the same: at a thickness of 10 nm — 23.5 nm, at 12.5 nm — 26 nm, at 15 nm — 24.5 nm. When the value of the second critical current is exceeded and the vortex leaves the edge of the disk in a thin magnetic layer in a thick one, a sharp decrease in the radius of the orbit is observed with its further increase to its maximum value. When the third critical current is reached, the vortex core in the thick magnetic layer goes beyond the STNO boundaries, as well as in the thin one. The maximum radius of motion for different thicknesses of the non-magnetic layer also slightly differs from each other. So, for a non-magnetic layer with thickness of 10 nm, the maximum radius equals 42 nm, at 12.5 nm — 42.5 nm, at 15 nm — 47 nm.

Figure 2 shows that as the value of the spin-polarized current increases, the frequency of stationary motion slightly decrease. With an increase in the thickness of the nonmagnetic layer, a decrease in the values of the frequencies of stationary motion is observed. The maximum value of the

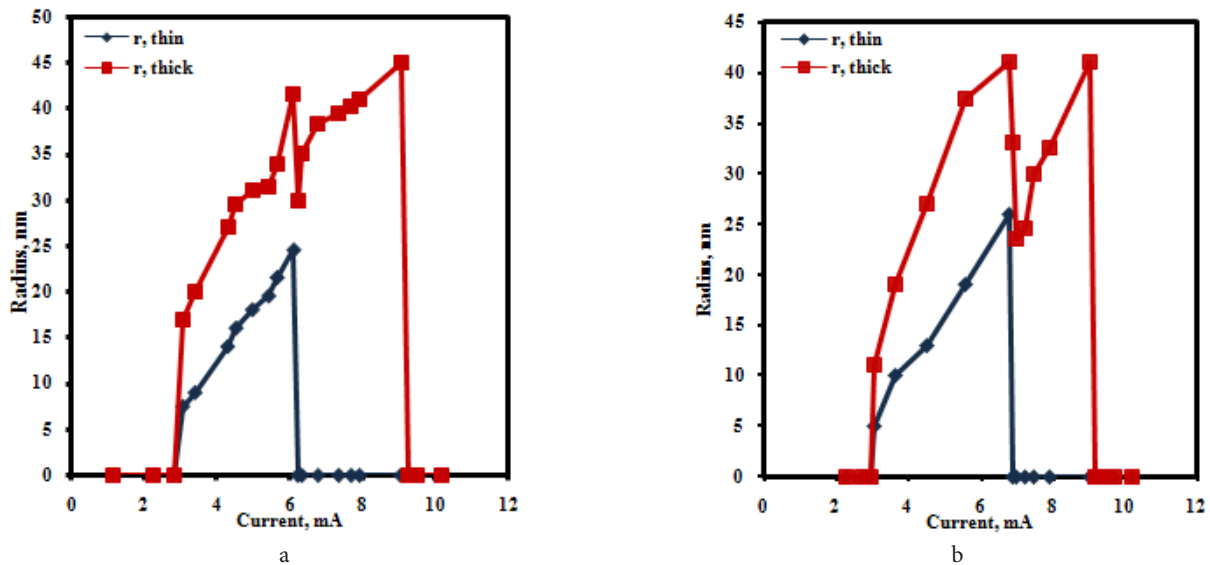


Fig. 1. (Color online) Dependence of the trajectory radius of vortices in thin and thick magnetic layers on the magnitude of the spin-polarized current for a non-magnetic layer with a thickness of 12.5 nm (a) and 15 nm (b).

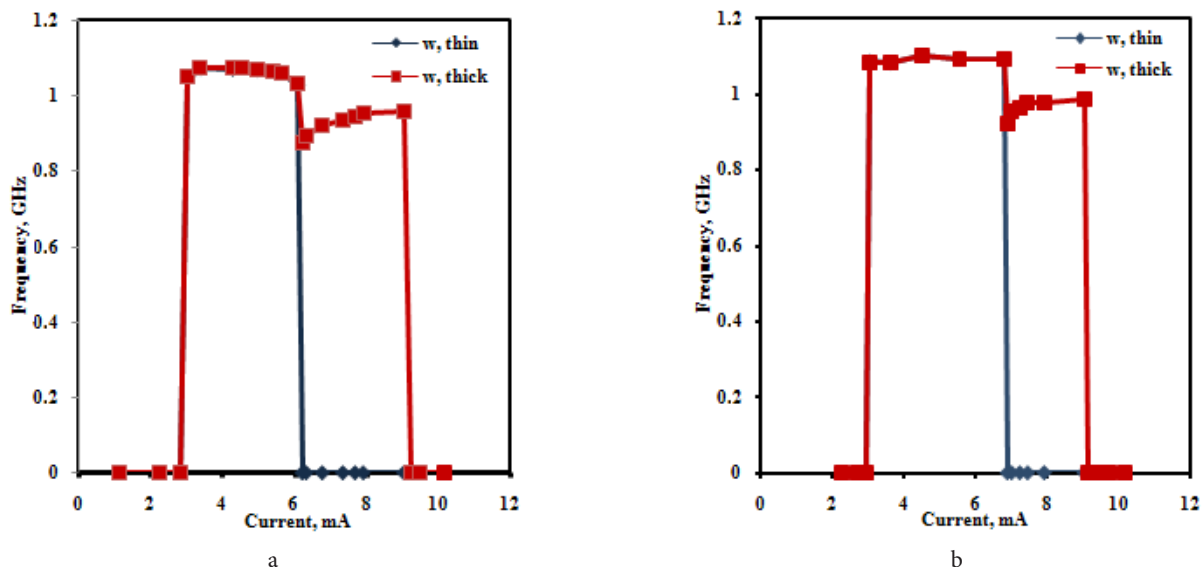


Fig. 2. (Color online) Dependence of the frequency of coupled oscillations of vortices in thin and thick magnetic layers on the magnitude of the spin-polarized current for a non-magnetic layer with a thickness of 12.5 nm (a) and 15 nm (b).

frequency of stationary coupled oscillations of vortices with a non-magnetic layer 10 nm thick is 1.109 GHz, at 12.5 nm — 1.095 GHz, at 15 nm — 1.076 GHz. At a current larger than the second critical one, the vortex in the thick magnetic layer switches to a new stationary mode of oscillation. The minimum value of this frequency at 10 nm is 0.925 GHz, 12.5 nm — 0.923 GHz, 15 nm — 0.861 GHz. In this case, there is a slight increase in frequency with increasing current.

There is an interesting feature has been found. At some points of current value (for example, with a non-magnetic layer thickness of 15 nm, these are 9.27 and 9.39 mA, and with a non-magnetic layer thickness of 12.5 nm, 9.16 mA) exceeding the value of the third critical current, a dynamic regime in a thin magnetic layer associated with the return of a vortex with a switched polarity to the disk. Further on, a stationary regime of coupled oscillations of vortices with antiparallel polarities was observed.

Table 1 shows that an increase in the thickness of the non-magnetic layer leads to a large decrease (by tens of percent) in the values of the first and second critical currents and a slight decrease in the value of the third critical current. The time of reaching the stationary regime of vortex oscillations nonlinearly decrease with increasing current, similarly to the dependence for the case of 10 nm, and has the same order of magnitude in time (see Fig. 3). It can be seen from Fig. 3 that a change in the thickness of the non-magnetic layer had little effect on the time it took for the vortex core to reach the stationary type of motion.

When the current value increases more than the value of the second critical value the departure of a vortex in a thin magnetic layer and the transition of a vortex in a thick magnetic layer to a new stationary orbit of a smaller radius is observed. The observed dynamics of vortices occurs similarly

to the case when a nanocylinder with a non-magnetic layer 10 nm thick was considered [12]. The dependence of the time of departure of the vortex from the thin layer on the magnitude of the applied current for the case of a non-magnetic layer of 12.5 and 15 nm is shown in Fig. 4. It is similar to the same dependence for the case of a nanostool with a non-magnetic layer of 10 nm and has the same order of magnitude in time (see Fig. 4). However, the increase in thickness significantly affected the time of “departure” of the vortex core beyond the STNO boundary. So, you can see that the “departure” time has increased by 10–15 units. With a further increase in the current higher than the value of the third critical current, as shown earlier [12], a regime with the disappearance of vortex states in both directions is observed. Note that in Fig. 3 times for different cases of non-magnetic interlayer thickness starting from 4 mA practically coincide. And in Fig. 4 times for different cases of non-magnetic interlayer thicknesses always do not coincide at the same current value. Interestingly, with a thicker nonmagnetic layer, the vortex core leaves the boundaries of the nanocylinder faster.

4. Conclusion

The influence of the thickness of a nonmagnetic layer on the coupled dynamics of two magnetic vortices in a spin torque nano-oscillator has been studied. The dynamics of vortex states in thick and thin magnetic layers at different values of current density is studied. The dependence of the frequency of stationary motion of vortices in thick and thin magnetic layers on the magnitude of the spin-polarized current density is found. A graph of the dependence of the radius of stationary motion of the vortex in thick and

Table 1. Dependence of the value of critical currents on the thickness of the non-magnetic intermediate layer.

Interlayer thickness	First critical current	Second critical current	Third critical current
10 nm	4.64 mA	7.35 mA	9.27 mA
12.5 nm	3.05 mA	6.89 mA	9.04 mA
15 nm	3.05 mA	6.33 mA	9.04 mA

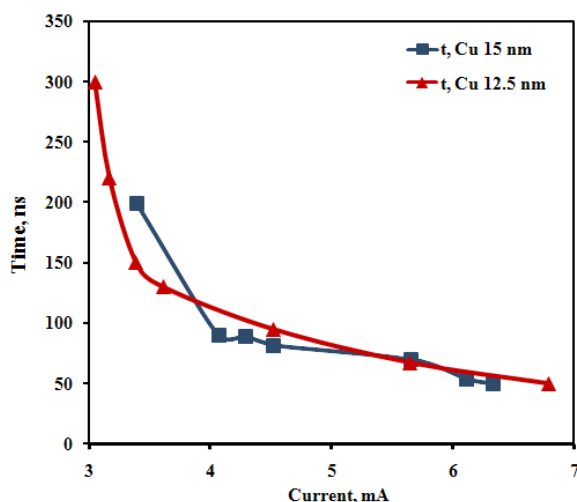


Fig. 3. (Color online) Dependence of the STNO exit time to the stationary mode of oscillations for different cases of non-magnetic layer thickness.

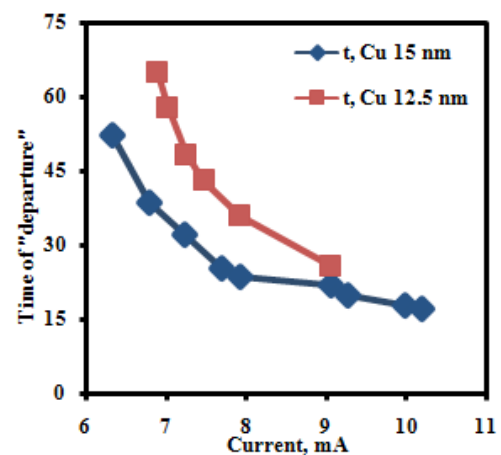


Fig. 4. (Color online) Dependence of the time required for the escape of a vortex from a thin magnetic layer on the magnitude of the applied current for various cases of the thickness of the non-magnetic layer.

thin layers on the magnitude of the spin-polarized current density is constructed. The obtained results are compared with the previously studied case of a non-magnetic layer of 10 nm. It has been shown that an increase in the thickness of the nonmagnetic layer leads to a large decrease (by tens of percent) in the values of the first and second critical currents and a slight decrease in the value of the third critical current. The time to reach the stationary regime of vortex oscillations and the time for the vortex to leave the thin layer decrease non-linearly with increasing current. At some points of current value exceeding the value of the third critical current, a vortex in a thin layer returned to the disk with switched polarity and a stationary mode of coupled oscillations of vortices with antiparallel polarities was observed.

Acknowledgements. V.V.M. thanks for the financial support of the State assignment of Russian Federation For The implementation of Scientific Research by laboratories (#075-03-2021-193/5 30.09.2021). K.A.Z. thanks for the financial supported RSF Grant No. 19-12-00432.

References

1. K. A. Zvezdin, E. G. Ekomasov. Phys. Metals Metallogr. 123, 201 (2022). [Crossref](#)
2. K. Y. Guslienko. Journal of Nanoscience and Nanotechnology. 8, 2745 (2008). [Crossref](#)
3. D. Yu, J. Kang, J. Berakdar, C. Jia. NPG Asia Mater. 12, 36 (2020). [Crossref](#)
4. J. Grollier, D. Querlioz, K. Y. Camsari, K. Everschor-Sitte, S. Fukami, M. D. Stiles. Nat. Electron. 3, 360 (2020). [Crossref](#)
5. S. Wittrock, P. Talatchian, M. Romera, S. Menshawy, M. J. Garcia, M.-C. Cyrille, R. Ferreira, R. Lebrun, P. Bortolotti, U. Ebels, J. Grollier, V. Cros. Appl. Phys. Lett. 118, 012404 (2021). [Crossref](#)
6. R. V. Verba, D. Navas, A. Hierro-Rodriguez, S. A. Bunyaev, B. A. Ivanov, K. Y. Guslienko, G. N. Kakazei. Phys. Rev. Applied. 10, 031002 (2018). [Crossref](#)
7. K.-S. Lee, M.-W. Yoo, Y.-S. Choi, S.-K. Kim. Phys. Rev. Lett. 106, 147201 (2011). [Crossref](#)
8. M. E. Stebliy, S. Jain, A. G. Kolesnikov, A. V. Ognev, A. S. Samardak, A. V. Davydenko, E. V. Sukovatitsina, L. A. Chebotkevich, J. Ding, J. Pearson, V. Khovaylo, V. Novosad. Sci. Rep. 7, 1127 (2017). [Crossref](#)
9. N. Locatelli, V. V. Naletov, J. Grollier, G. Loubens, V. Cros, C. Deranlot, C. Ulysse, G. Faini, O. Klein, A. Fert. Appl. Phys. Lett. 98, 062501 (2011). [Crossref](#)
10. K. Y. Guslienko, K. S. Buchanan, S. D. Bader, V. Novosad. Appl. Phys. Lett. 86, 223112 (2005). [Crossref](#)
11. N. Locatelli, A. E. Ekomasov, A. V. Khvalkovskiy, S. A. Azamatov, K. A. Zvezdin, J. Grollier, E. G. Ekomasov, V. Cros. Appl. Phys. Lett. 102, 062401 (2013). [Crossref](#)
12. A. E. Ekomasov, S. V. Stepanov, K. A. Zvezdin, E. G. Ekomasov. Physics of Metals and Metallography. 118, 328 (2017). [Crossref](#)
13. S. S. Cherepov, B. C. Koop, A. Y. Galkin, R. S. Khymyn, B. A. Ivanov, D. C. Worledge, V. Korenivski. Phys. Rev. Lett. 109, 097204 (2012). [Crossref](#)
14. E. Holmgren, A. Bondarenko, B. A. Ivanov, V. Korenivski. Phys. Rev. B. 97, 094406 (2018). [Crossref](#)
15. V. Sluka, A. Kakay, A. M. Deac, D. E. Burgler, C. M. Schneider, R. Hertel. Nature Communications. 6, 6409 (2015). [Crossref](#)
16. A. Hamadeh, N. Locatelli, V. V. Naletov, R. Lebrun, G. Loubens, J. Grollier, O. Klein, V. Cros. Phys. Rev. Lett. 112, 257201 (2014). [Crossref](#)
17. A. E. Ekomasov, S. V. Stepanov, K. A. Zvezdin, E. G. Ekomasov. J. Magn. Magn. Mat. 471, 513 (2019). [Crossref](#)
18. Y. Gaididei, V. P. Kravchuk, D. D. Sheka. International Journal of Quantum Chemistry. 110, 83 (2009). [Crossref](#)
19. K. Y. Guslienko, O. V. Sukhostavets, D. V. Berkov. Nanoscale Research Letters. 9, 386 (2014). [Crossref](#)
20. A. E. Ekomasov, S. V. Stepanov, E. G. Ekomasov. Letters on Materials. 6 (1), 46 (2016). [Crossref](#)
21. E. G. Ekomasov, S. V. Stepanov, K. A. Zvezdin, N. G. Pugach, G. I. Antonov. Phys. Metals Metallogr. 122, 197 (2021). [Crossref](#)
22. D. V. Berkov, J. Miltat. Journal of Magnetism and Magnetic Materials. 320, 1238 (2008). [Crossref](#)
23. J. Leliaert, J. Mulders. J. Appl. Phys. 125, 180901 (2019). [Crossref](#)
24. G. D. Loubens, A. Riegler, B. Pigeau, F. Lochner, F. Boust, et al. Phys. Rev. Lett. 102, 177602 (2009). [Crossref](#)